

First measurement of the guide coil field and the magnetic environment in the new NPD γ cave at LANSCE.

Bernhard Lauss
UC Berkeley

February 6, 2004

1) General setup of stand and guide coils

The magnetic field of the NPD γ experiment is produced with 4 guide coils mounted in double Helmholtz condition. Fig.1 shows the distances of the electrical centers calculated to meet the required homogeneity standards.

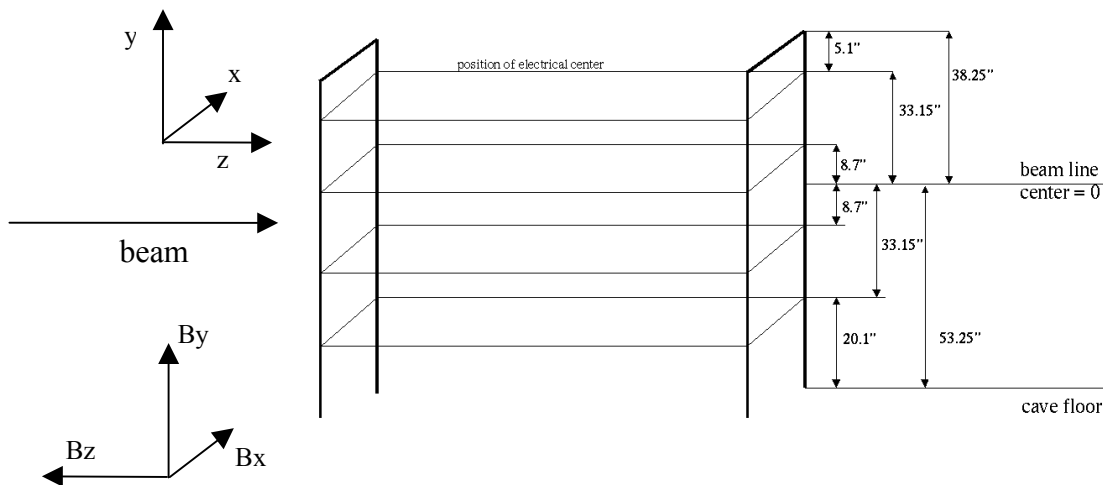
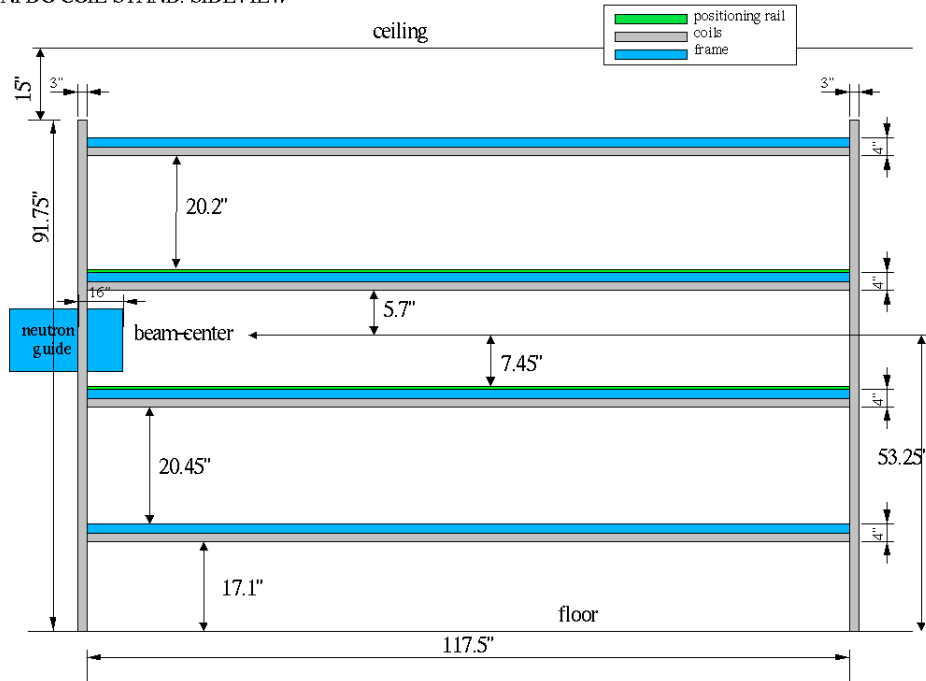


Fig.1: Positions of electrical centers of guide coils in double Helmholtz mounting. Definition of coordinate system and positive field directions.

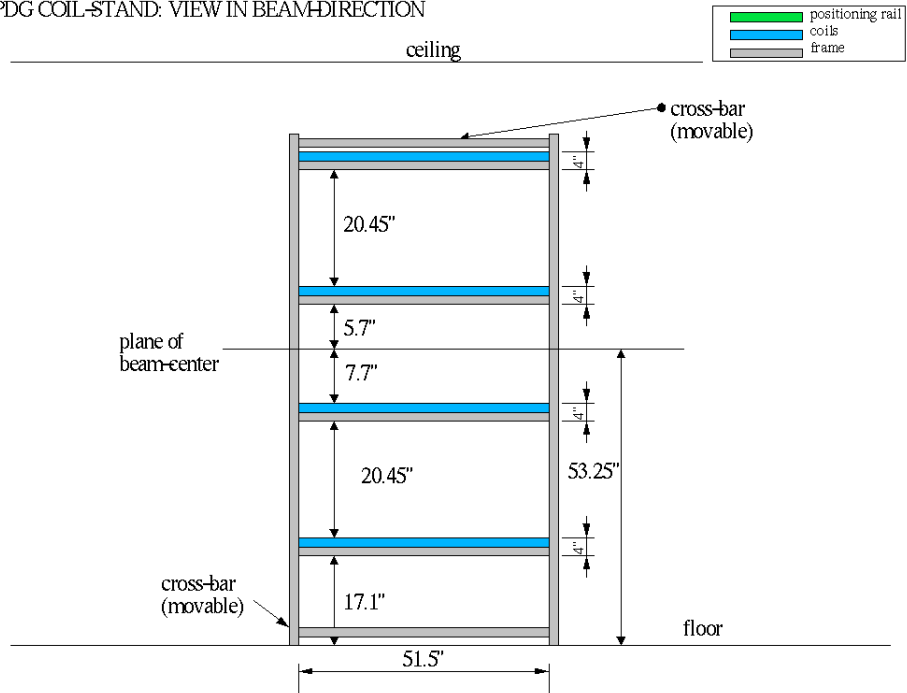
The coils are physically wound on aluminum extrusions. These are mounted on an aluminum stand made from 8020 industrial frame parts. All screws, nuts and washers were tested to be non-magnetic (Permeability $<1.01 \mu$).

In Fig.2 the exact dimensions of the mounted coils on the frame are shown. The mounting was done with respect to the beam height of 53.25" above cave ground and with respect to the beam exit flange of the neutron guide. Its front plate reaches 16" inside the coil stand. All cross-bars were leveled. The cave floor is not leveled perfectly.

NPDG COIL-STAND: SIDEVIEW



NPDG COIL-STAND: VIEW IN BEAM DIRECTION



BL/03/11/03

Fig.2: Side view and front view of the coil stand with indicated measures and distances used for the setup.

Figure 3 shows an actual photo of the finished NPD γ cave with the coil stand and coils as mounted in January 2004. The neutron guide is penetrating the front wall.



Fig.3: Coil stand and coils in the NPD γ cave with the detector table already in place and the neutron guide reaching inside.

The presently installed setup and system consists of the following items:

Field creation:

- Coils: 2 inner coils: 21+2+1 windings + 15 shim windings
2 outer coils: 36+2+1 windings + 15 shim windings
- Stand
- Danfysik Magnet Power Supply 858 - System 8000 (main coil)
- Agilent Power Supply E3644A (80W) (shim coils)
- 2x Agilent Power Supply E3648A (100W) (shim coils)

Field measurement:

- 2x Bartington 3-axis flux gate magnetometer MAG-03
- Bartington flux gate Data Acquisition Module (MAG-03 DAM)
- 2x Optical Multiplexer - 8-channel RS232 Fiber Optic Micro-Mux TC1880
- 8-port RS-232 PCI Serial Board ESC-100D
- Personal Computer (Compaq Pentium, running Labview under Windows XP professional)

2) Flux gates as field measurement devices

Two rectangular calibrated and aligned 3-axis flux gate magnetometers made by Bartington are used for the field measurement. The alignment of the 3 sensors within one probe are better than 0.1 degree as is the alignment to the base plate of the flux gates. A short description of the working principle of flux gates is given in Appendix A.

The flux gates can be mounted on a precision machined cross-bar with reproducible 25 pin locations. This cross-bar can be mounted on the positioning rails of the 2 inner coils which have 43 precision pin holes 2" apart from each other.

In the presented measurements we used 2 flux gates mounted in different positions. The positions were measured as given in Table 1, with the cross-bar located with pins 42 and 43 on the lower central coil (Probe 1 and 2) and on the upper central coil (Probe 3 and 4). The coordinate system's point of origin is at the beam center on the exit flange, with x being the horizontal axis from left to right (looking upstream), y being the vertical axis pointing up, z is the beam axis pointing downstream, as defined in Fig. 1.

The pin holes on the rail and cross-bars are all 2" apart. Table 2 gives the distances in position between the mounted probes. The positions of the sensors within the probe is not taken into account in the position given in the field plots. These sensor positions, as given in the Bartington manual, are in the center of the probe at the following distance d from the front plate: Bx-sensor: d = 40 mm; By-sensor: d=10mm; Bz-sensor: d=25 mm.

	X (mm)	Y (mm)	Z (mm)	position
center of beam on exit flange	0	0	0	
Probe position 1	5	-12	30	central
Probe position 2	-122	-171	15	lower left
Probe position 3	5	81	21	upper central
Probe position 4	112	270	41	upper right

Table 1: Definition of probe positions.

	dx (mm)	dy (mm)	dz (mm)
d 1-2	127	159	15
d 1-3	0	93	9
d 1-4	107	282	11

Table 2: Definition of distances between the individual probe positions.

3) Measurements with field coils OFF – ambient field in the cave

In the following we plot the measurements of the magnetic field as obtained in the cave with the field coils off. Plotted are B_x , B_y , and B_z . For B_x and B_z we plot only probe 1 as the relative alignment of probe 1 and 2 seems to have shifted during the measurement. Consequently the total field B_{tot} stayed the same, but the axes B_x and B_z changed differently. The B_y axis was fixed with screws and did not shift. All plots positions are along the beam axis starting at the beam exit flange.

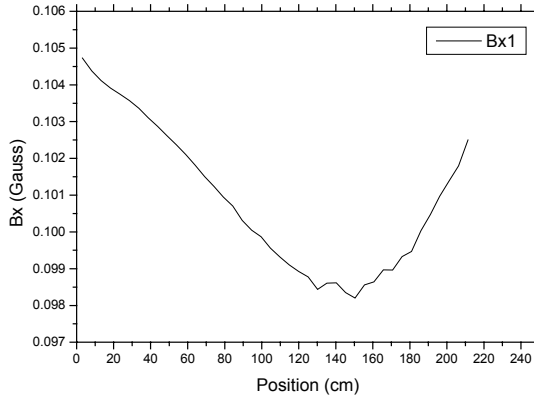


Fig.4: B_x values measured with coils off.

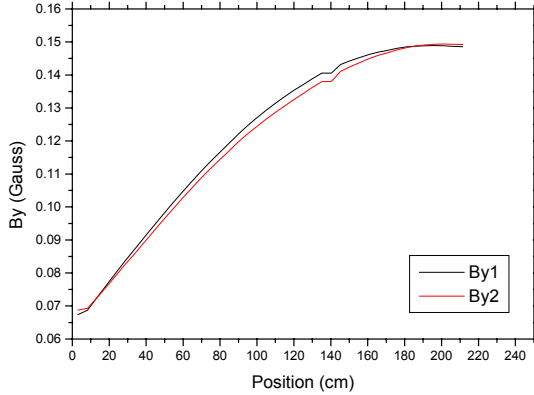


Fig.5: B_y values measured with coils off in position 1 and 2.

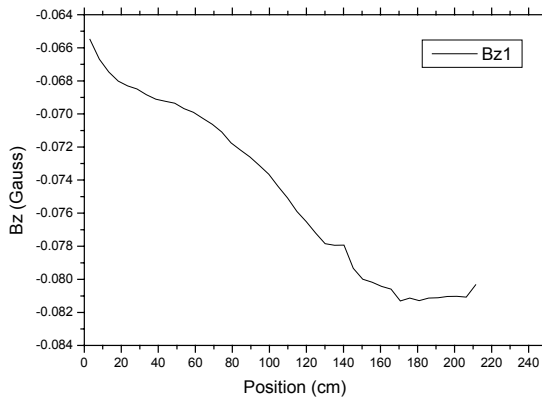


Fig.6: B_z values measured with coils off.

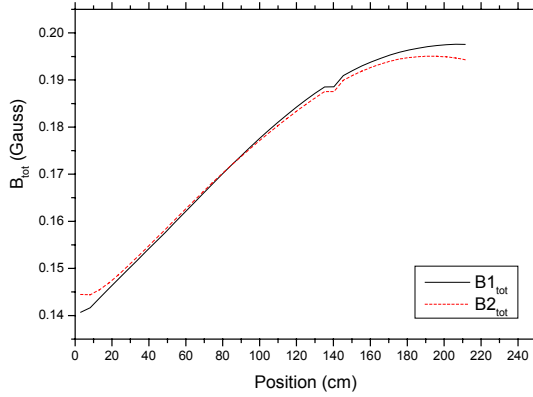


Fig.7: Btot values as calculated from the 3 axis values in probe positions 1 and 2.

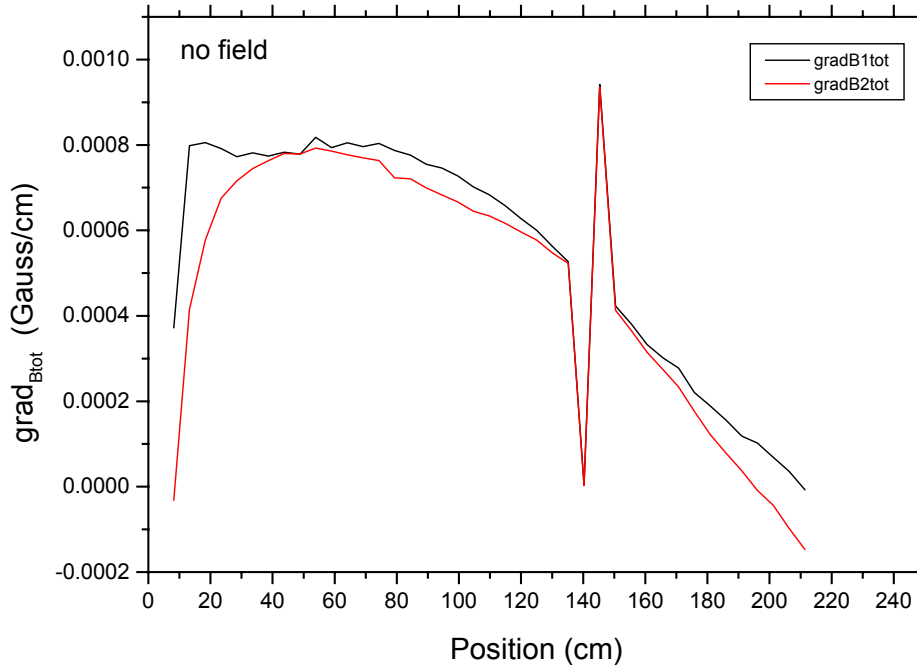


Fig. 8: Gradient of Btot for probe position 1 and 2. The gradient is calculated by subtracting two subsequent measurements 2” apart.

The field measurement with the coils off reveals the rest magnetization of the cave steel walls which dominates over the probably fully shielded earth field which should show up as constant value easily shimmed. The individual axes and Btot show a smooth increase or decrease of the field. The Btot gradient shows a spike at the location of the back steel rail of the detector table. However the gradient is well under 1mGauss/cm for all the positions.

4) Measurements with guide coils ON

After a 2 day tuning process in order to decrease the field gradient along the beam axis we finally run the coils with a total current of 18 Amps in the main windings (using the Danfysik power supply) and 4 Amps (with an Agilent E3644A power supply) in the outer 15 shim windings. The current ratio of outer to inner coils was 2.016.

a) Absolute field values

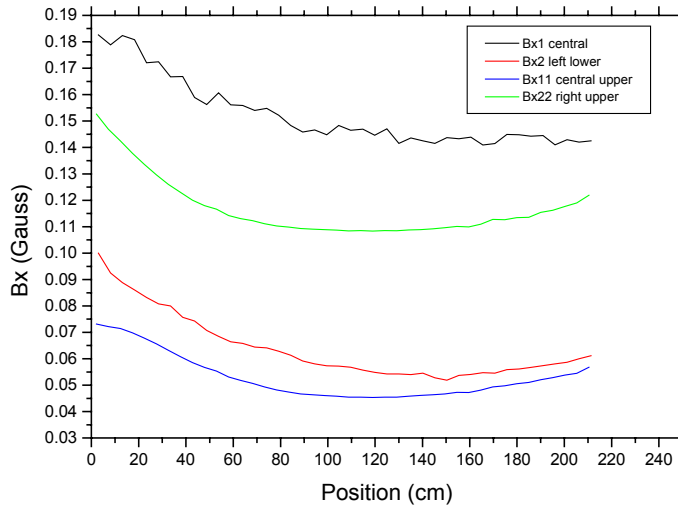


Fig.9: B_x field measured in 4 positions as given in table 1 with coils on.

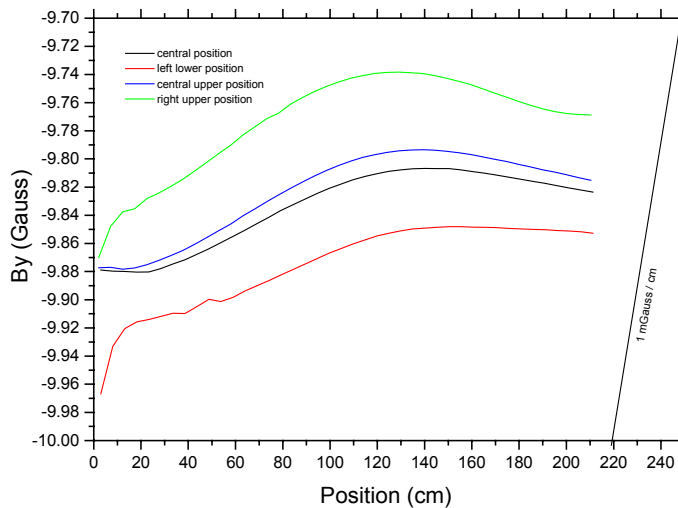


Fig.10: B_y field measured in 4 positions as given in table 1 with coils on. The allowed gradient of 1mGauss/cm is sketched on the right.

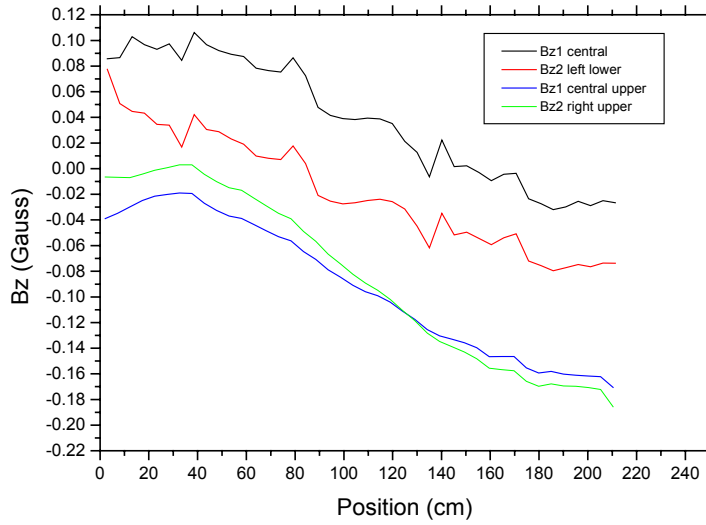


Fig.11: Bz field measured in 4 positions as given in table 1 with coils on.

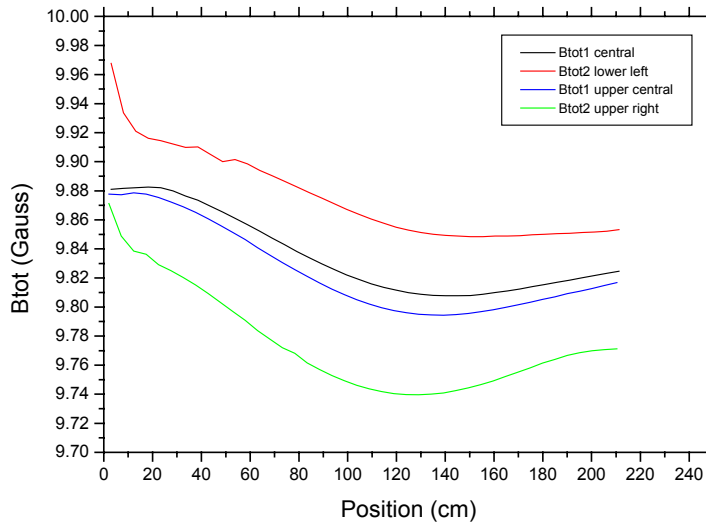


Fig.12: Btot field measured in 4 positions as given in table 1 with coils on.

The obtained field values with the coil on are well within specs and show a mainly smooth behavior along the beam axis. Clearly observable is a sharp field distortion right after the beam exit flange which might be due to magnetized materials in the neutron guide, namely the steel pipe. Some spikes are clearly visible in the Bz component of the field. Two of those can be matched to the beginning and the end of the motor which is driving the detector table, a clearly magnetizable material and the two steel rails on this table. As there are no constant field values in x and z, no simple shim coils can be used to even out these field components.

In order to see how well the experimental requirements concerning field gradients are matched, we look at the plotted field gradients in the following subchapter.

b) Calculated field gradients of one probe along the beam axis

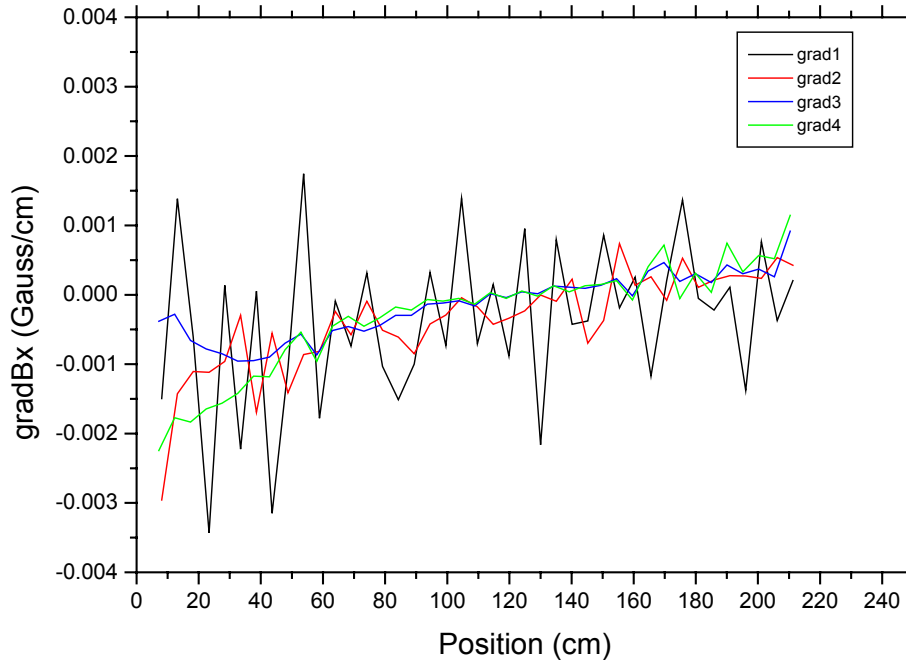


Fig.13: Gradient of Bx along the beam axis measured independently in the 4 probe positions. The large fluctuations of probe 1 (grad1) are probably due to positioning inaccuracies.

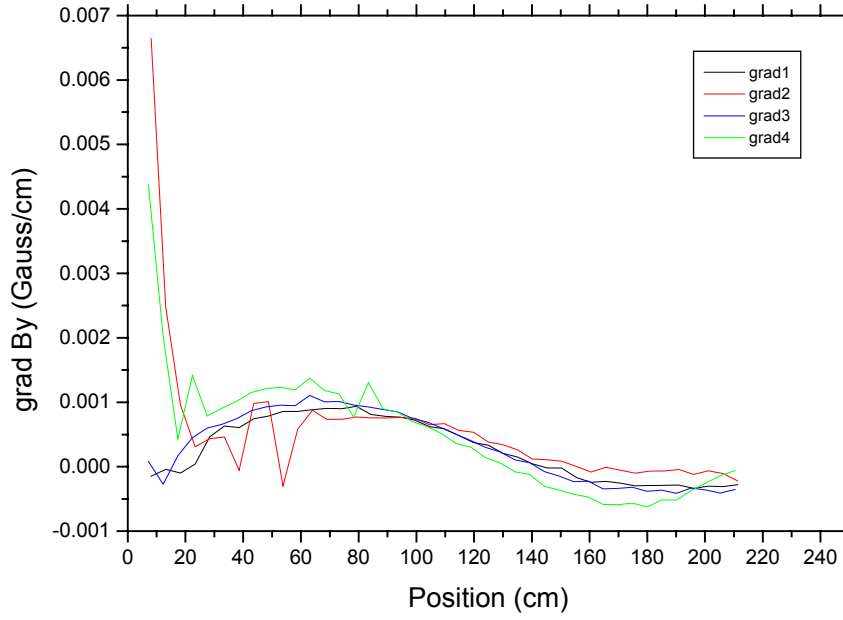


Fig.14: Gradient of B_y along the beam axis measured independently in the 4 probe positions. Clearly we see an influence of the neutron beam guide at the end flange. Most of the range is well below the required 1mGauss/cm.

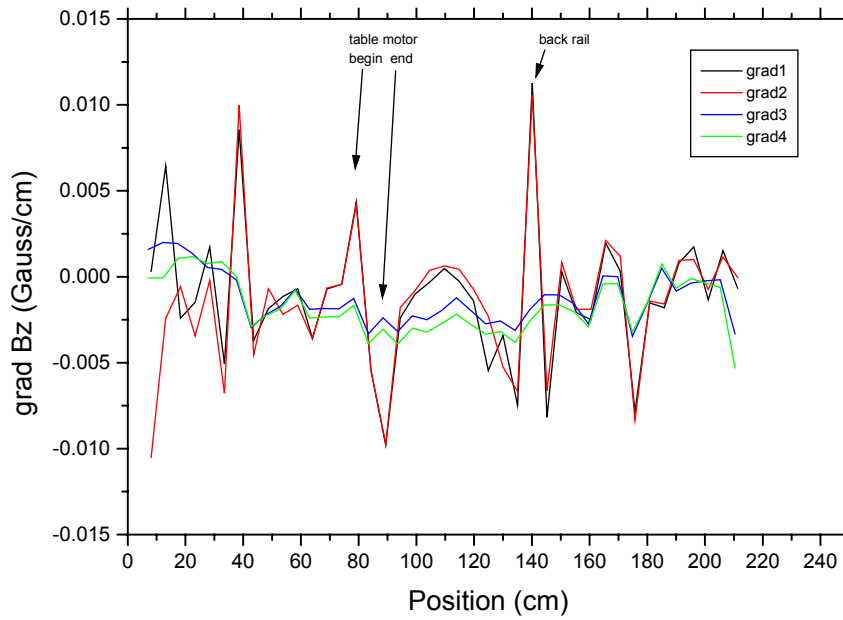


Fig.15: Gradient of B_z along the beam axis measured in the 4 probe positions. Large variations can be seen in positions which are identified with the detector table motor and steel rails.

Figures 13-15 displaying the field gradients show spikes in the 2 non-coil-field axes. While some spikes are presently unexplained, but most likely due to a misalignment of the probes, the spikes in the location of the detector table motor and steel rails have been observed during several repeated scans. Fig.16 shows this repeated monitoring. Figure 17 shows the approximate locations of the equipment items along the measured coordinates to allow for an easy cross-check.

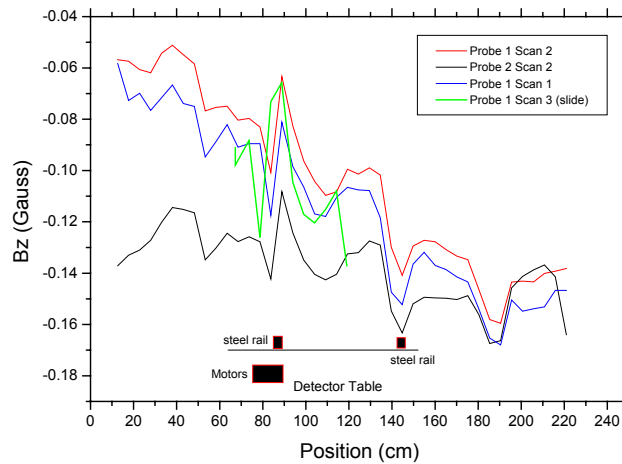


Fig.16: Several scans across the detector table reveal its influence on the B_z component of the field. The approximate location of the steel rails and the table moving motors is indicated.

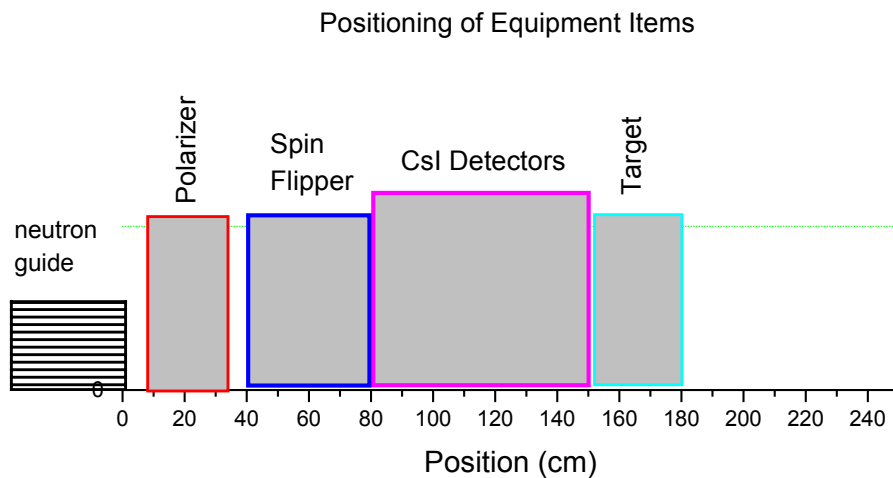


Fig.17: The positions of the relevant equipment in the same coordinates as shown on all field and gradient plots.

The field gradients measured along the beam axis in 4 different positions and for all 3 field directions are below the targeted value of 1mGauss/cm. However, the spiky structure in Bx and Bz can be related to some magnetizable material still present within the field stand, which should be replaced or shielded. The field immediately after the neutron guide exit flange due to the steel in the tube seems to have a large gradient. The influence on the polarizer should be studied.

The gradients calculated between the various probes are presently very large. This suggests that the probes were not aligned perfectly to each other and Bx and Bz were influenced from the much larger By field. Consequently these gradients have to be remeasured in a way which guarantees the alignment of the probe during the position change (see chapter 7 and 8).

5) Stability of field and flux gates measured with coils OFF

The field measurement was pursued for one night with coil current off in order to understand the stability of the flux gate measurement and the behavior of the cave environment. Figures 18-20 show the Bx, By and Bz fields observed.

The general behavior of Bx and Bz is very stable, and the structure with many spikes, which was observed in the test measurements at Berkeley, is not present. This is clearly a fact of the good shielding cave walls and the lower environmental noise at the Los Alamos Lab.

The large change around 9:00 am can be attributed to electrical workers starting to work in the cave, probably pushing the coil stand, which moved the probe a little.

The By field behavior is clearly different, as it shows a decrease over several hours which reflects the relaxation of the magnetization in the steel of the cave walls. The field was on and only turned off shortly before this measurement. Two different exponential decay time constants of 55 minutes and 430 minutes are present.

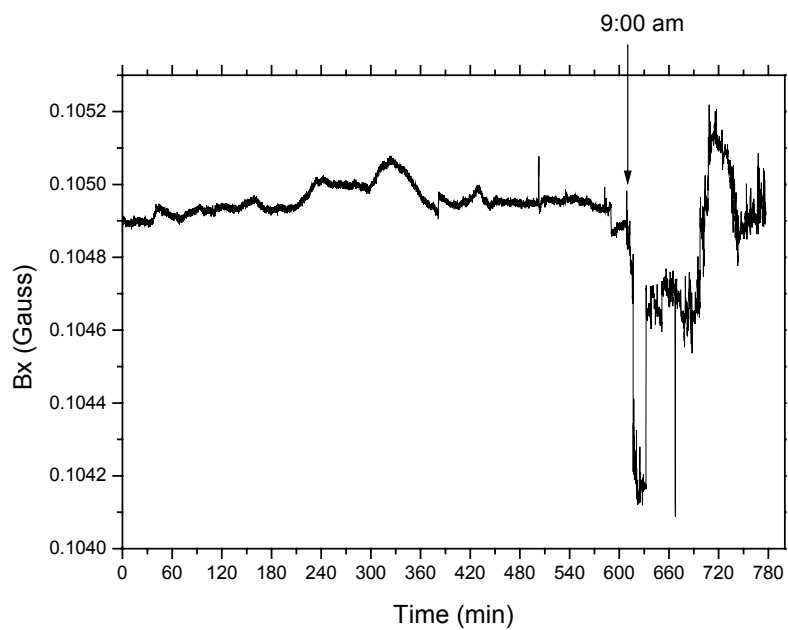


Fig.18: Bx field stability with coils off.

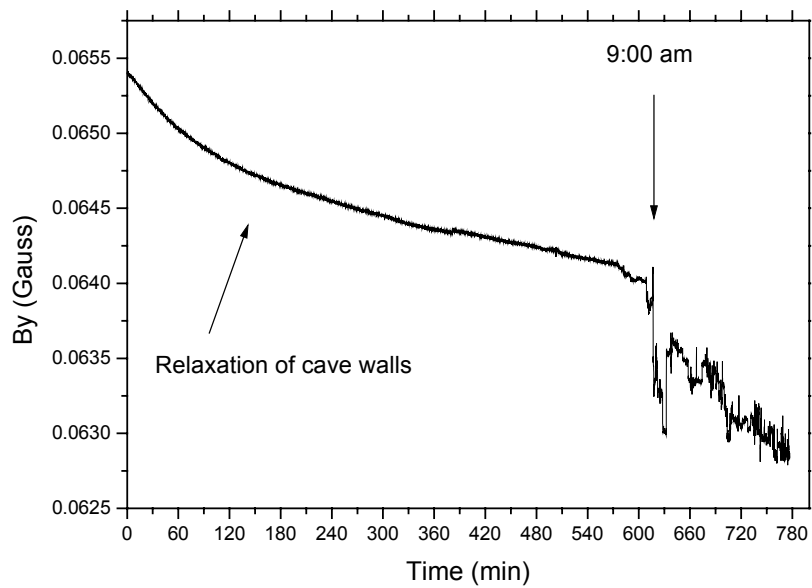


Fig.19: By field stability with coils off.

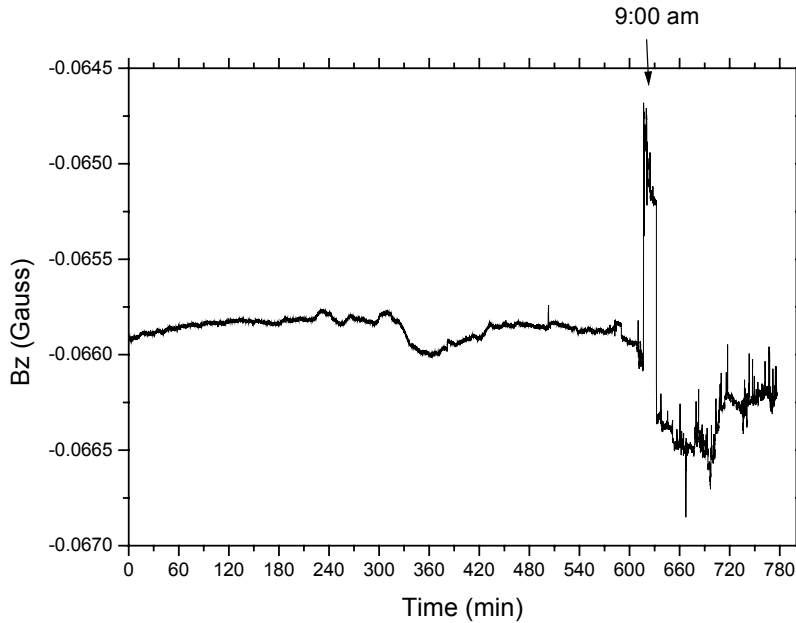


Fig.20: Bz field stability with coils off.

The noise of the flux gates is below 0.01 mGauss and the field stability is below 0.1 mGauss. The small drift very likely a temperature effect. Even small bumps at the stand change the probe/field direction and can be detected. Relaxation of the cave wall magnetization creates an observable effect.

6) Stability of field and flux gates measured with coils ON

Having established the stability of the field and of the flux gates with coils off, the field was turned on to ~10 Gauss and its stability was monitored for one night. The observed behavior of the field components is displayed in Figures 21-23.

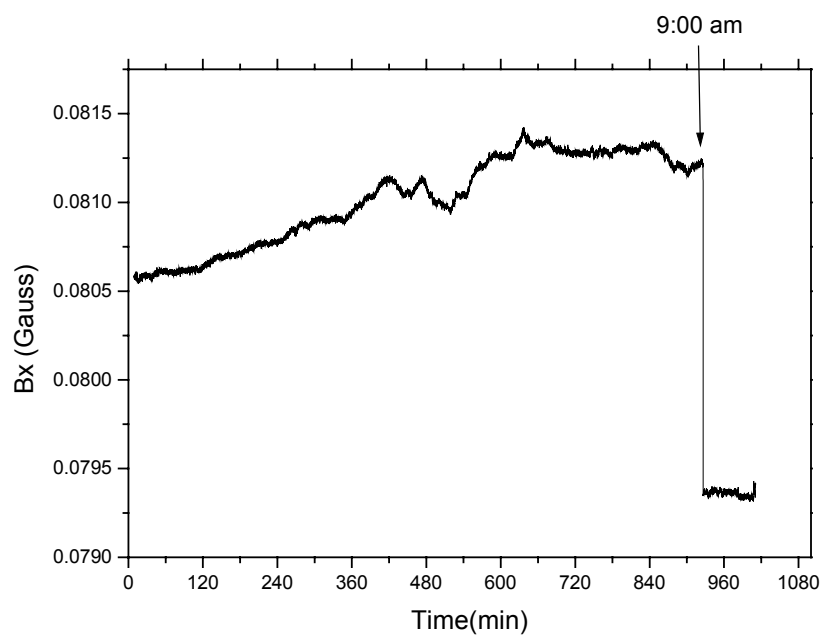


Fig.21: B_x stability with field coils on.

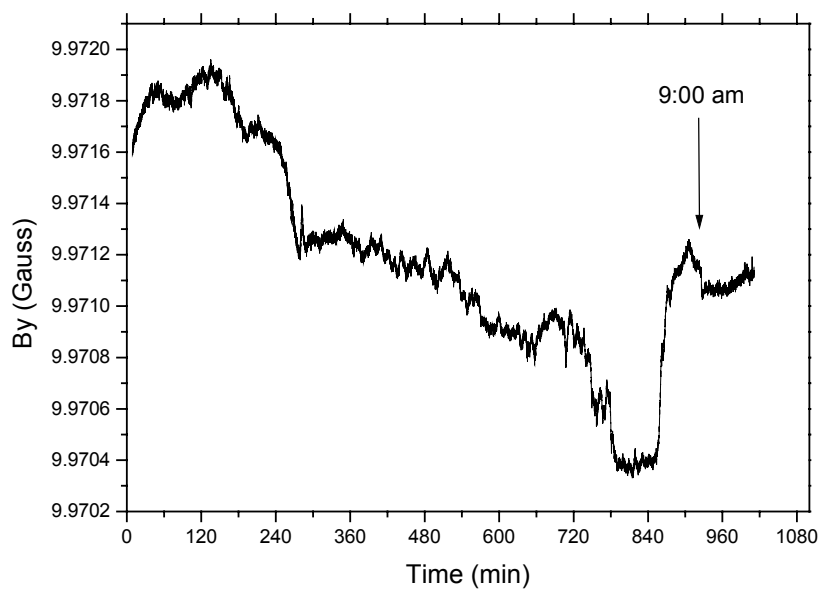


Fig.22: B_y stability with field coils on.

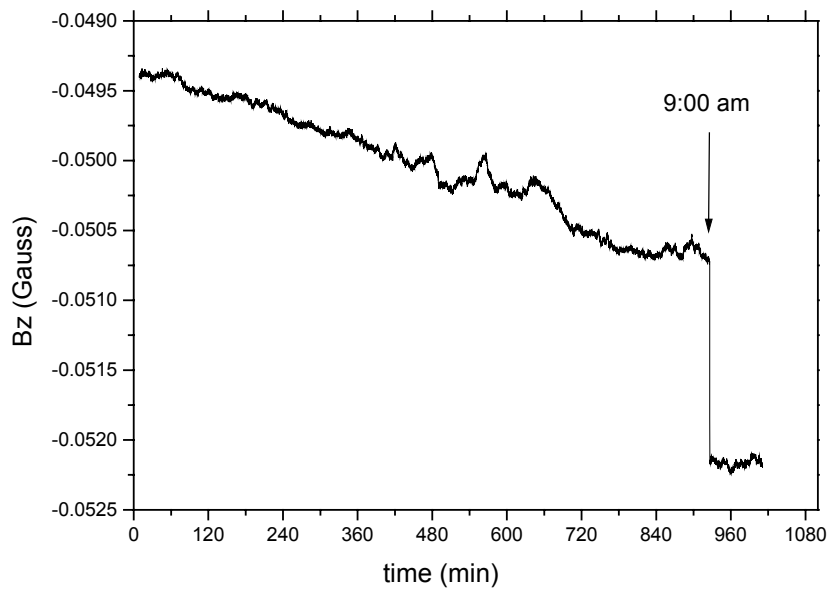


Fig.23: Bz stability with field coils on.

On the time scale of 10 hours the stability seems stable within a mGauss, but clearly a small drift of either the probe (or the coils) is visible, which could be caused by the probe slowly turning due to changing temperature or releasing screws, or the field coils changing size due to temperature effects. Clearly a longer observation period is needed to find the cause. However, I think that also the necessity of a controlled temperature in the environment of the cave is demonstrated. The large jump around 9:00 am is again due to people entering in the cave.

7) Field scan in the spin flipper and ^3He polarizer positions

In order to check the field distribution on the important places of the spin flipper (cross-bar at 18 cm, measured downstream from the neutron guide exit flange) and ^3He polarizer (cross-bar at 64 cm), horizontal field scans orthogonal to the beam direction were recorded. Fig. 24 (position of spin flipper) and Fig.25 (position of ^3He polarizer), display on the following 2 pages the measured fields.

The left column shows the horizontal position dependence of B_x , B_y , B_z and calculated B_{tot} while moving the flux-gate over the investigated area. The largest obtained gradients for each direction is indicated, the largest one being 3.1 mGauss/cm. To interpret this gradient, read also the next chapter on the measurement error.

In Fig. 24 and 25 the right column shows the coincident measurement with a flux-gate fixed in position 17.5 cm on the cross-bar (left from beam center) for control reasons. Note that in the control measurement 1mGauss fluctuations appear. The position of 33 cm marks the center of the coils in x-direction.

Fig.24 (next page): Scan of B_x , B_y , B_z and calculated B_{tot} in the position of the spin flipper together with coincident a control measurement with probe 2 at a fixed cross-bar location. Note that position refers to position in x across the magnet, coil center is at 33 cm.

Fig.25 (two pages ahead): Scan of B_x , B_y , B_z and calculated B_{tot} in the position of the ^3He polarizer together with coincident a control measurement with probe 2 at a fixed cross-bar location. Note that position refers to position in x across the magnet, coil center is at 33 cm.

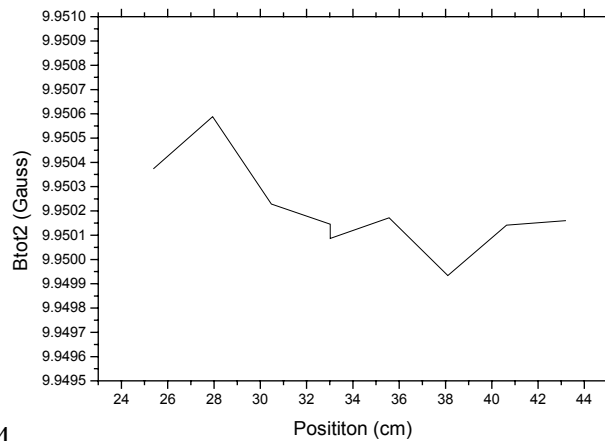
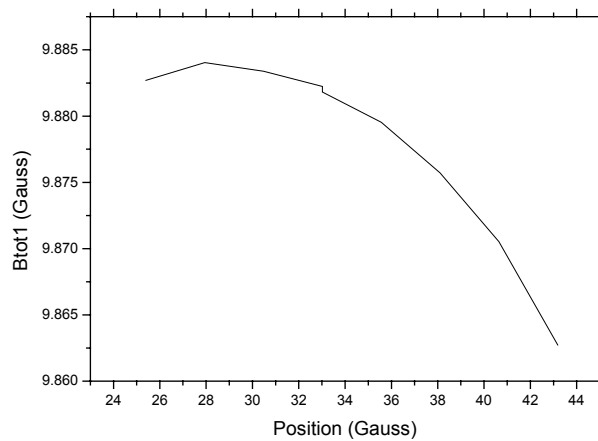
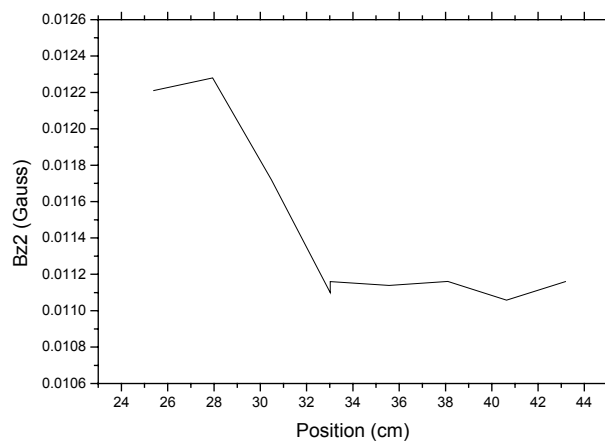
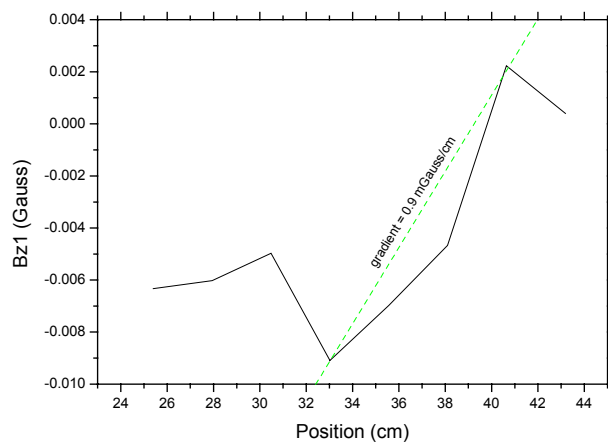
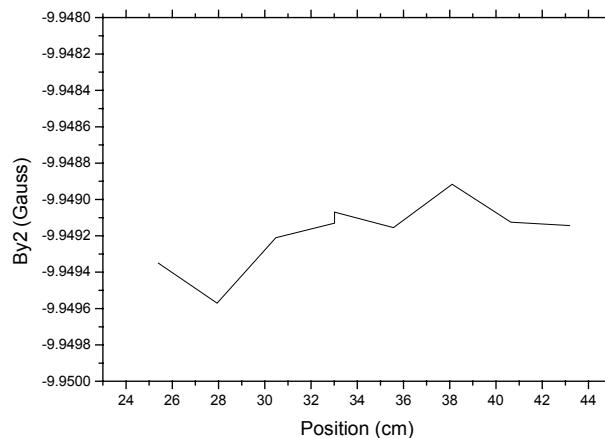
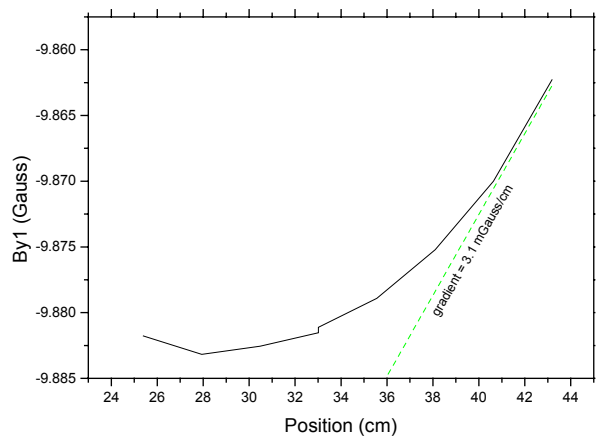
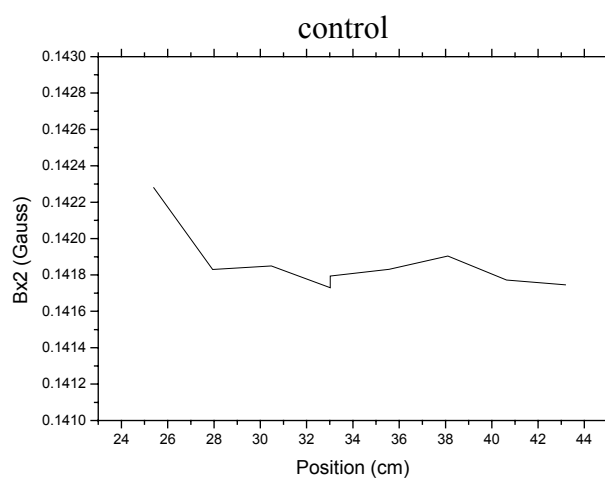
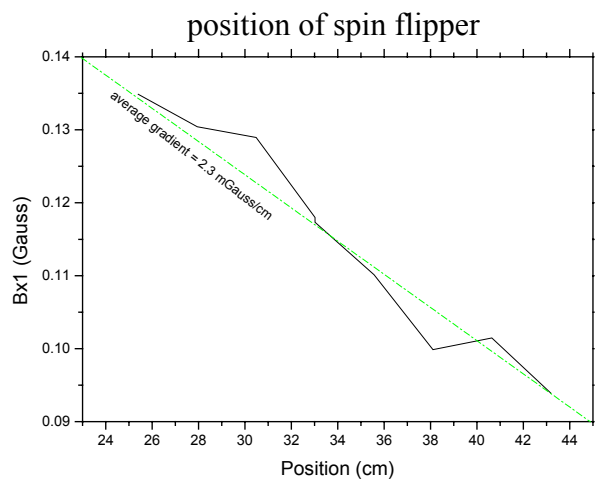


Fig.24

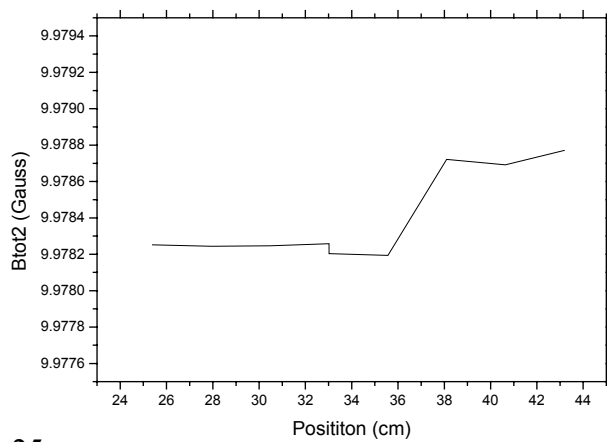
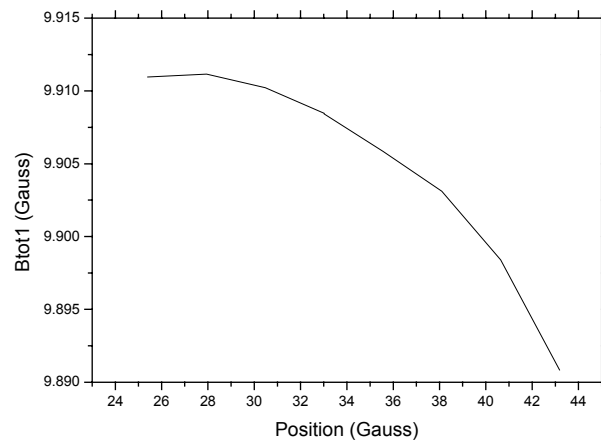
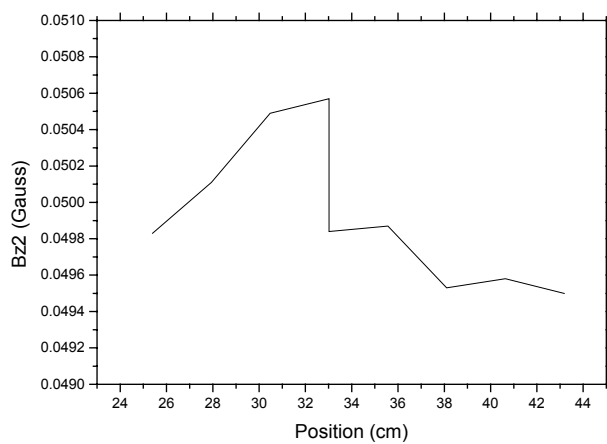
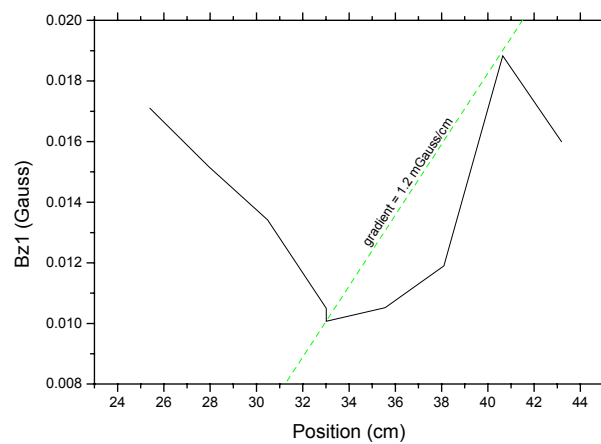
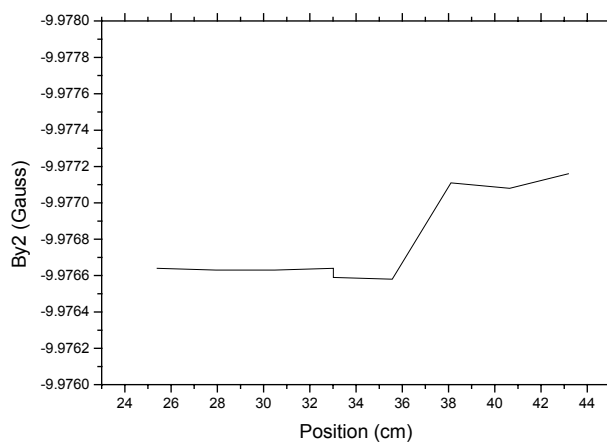
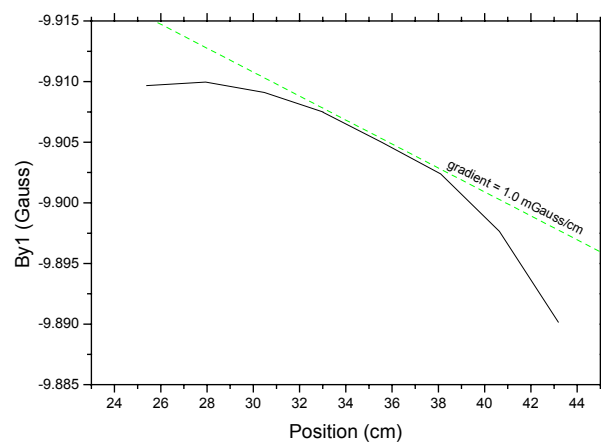
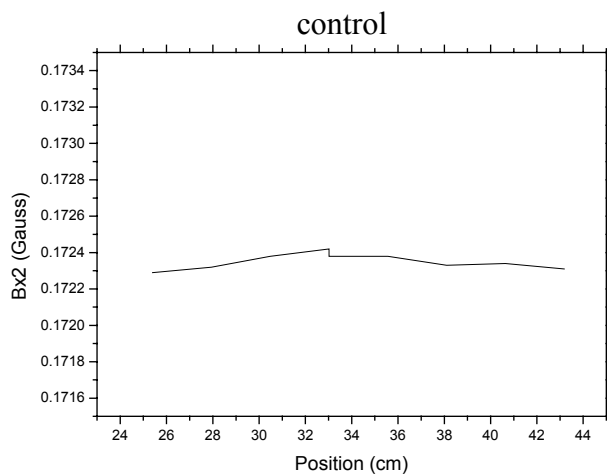
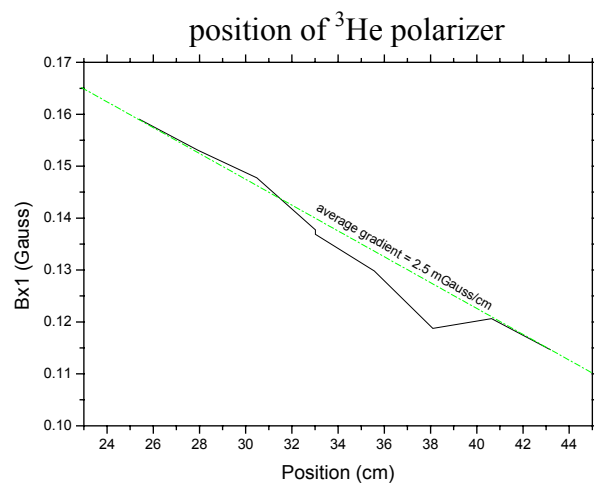


Fig.25

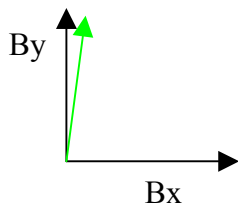
8) Field measurement errors

When interpreting the measurements given in this note one should always have in mind that:

1. The flux gates magnetometers are extremely sensitive devices with resolution of better than 0.01 mGauss in all 3 axes. Consequently a small skew of the probes already influences the measurement enormously.
2. The field created with the guide coils is a factor 100 larger than the field in the 2 other dimensions. Consequently, a small misalignment between the 4 large coils, which have been well leveled and aligned with standard tools available at LANSCE, might cause larger Bx and Bz values and large Bx and Bz gradients. A perfect alignment would minimize those contributions.

The following simple calculation shows the large sensitivity of the presented measurements to both error contributions.

Given a perfectly orthogonal system with $B_x=0$, $B_y=10000$ mGauss, $B_z=0$.
We skew this system by a tiny angle in one axis in order to split the field into



$$B_x = 1 \text{ mGauss} \Rightarrow B_y = \sqrt{10000^2 - 1} \text{ mGauss}, B_z = 0$$

This means that the system is only skewed by an angle of 0.006° , better illustrated by the height of 150 micron (6mil) one has to raise the probe (length 15cm) on one side to obtain a 1 mGauss mis-measurement. The same idea applies to the alignment of the 4 coils, which consequently should be better than 0.4 mm over the whole coil length.

The large gradients along Bx and Bz can, at this early time after the first installation and first alignment of the coil stand be an artifact of necessary further coil alignment and/or necessary better flux gate magnetometer positioning and mounting during measurements.

The fact that a tiny fluctuation around 10 Gauss is a relative small error in comparison to the same fluctuation at 0.1 Gauss, together with the better fixation of the probes in y direction, creates the smooth appearance of all plotted field scans along the beam axis.

9) Summary

The NPD γ guide coils were successfully installed in the experimental cave and a 10 Gauss field was reached with stable running conditions.

Overall the field gradients are within or close to specifications. Clearly the precision of the field scan and the guide coil alignment can be improved.

Magnetizing items interfering with field homogeneity were clearly observed and should be replaced.

To guarantee overall running stability within 1 mGauss over days one has to monitor and control the temperature of the cave, bearing in mind that the coil and supplies already create ~ 1 kW of power.

The field dependence on x, y and z should be remeasured carefully, especially with all the experimental equipment in place.

The observed non-constant background fields do not allow a simple shimming solution with coils at the end of the stand.

Acknowledgments

Special thanks go to **Rob Mahurin** for his help with the setup work and many measurements, and especially his weekend contributions. **Seppo Penttilä**'s help, suggestions and support is gratefully acknowledged.

Appendix A: Short description of flux gate working principle:

A flux gate is made out of two iron-like cores, primary coil, and secondary coil. The primary coil is wound around the two cores in series in opposite directions. The secondary coil is wound in the opposite direction of the primary one as shown in Fig.26.

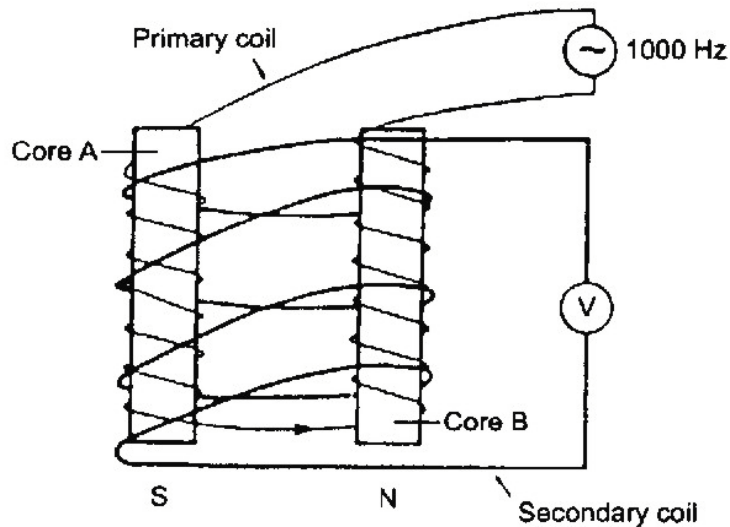


Fig.26: Sketch of the coil windings of a flux gate magnetometer.

An alternating current is passed through the primary coil producing a magnetic field that drives up each core to saturation. Once reached saturation, the core cannot magnetize any further. The magnetometer's material in the cores saturates every half cycle. Because of the opposite directions in the primary coil the net voltage induced in the secondary coil without a present magnetic field is zero. An external magnetic field parallel to the direction of the core saturates one of the cores faster, which is already partially saturated at the start of a cycle. Consequently the voltage in the secondary coil does not cancel. This behavior is sketched in Fig. 27.

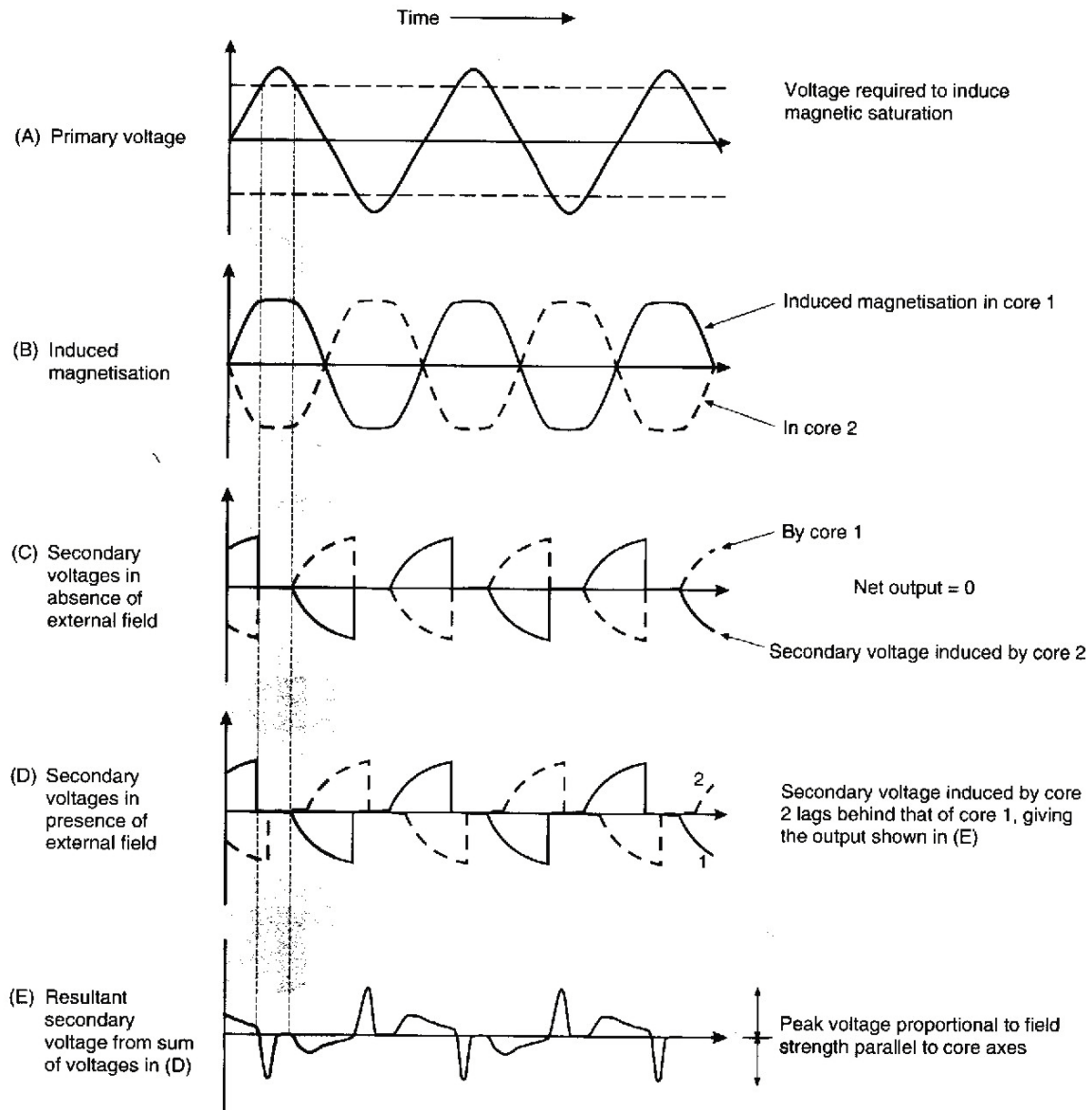


Fig.27: Voltages in a flux gate with and without presence of a magnetic field. In (C), the two dotted lines add and cancel each other out to give a zero net voltage, but in (D), the shift in the dotted line creates a net voltage that can be detected.